Journal of Materials Chemistry

Dynamic Article Links

Cite this: *J. Mater. Chem.*, 2012, **22**, 20831

www.rsc.org/materials

FEATURE ARTICLE

Semiconductor nanowires self-assembled from colloidal CdTe nanocrystal building blocks: optical properties and application perspectives

Yury P. Rakovich,[ab] Frank Jäckel,[c] John F. Donegan[d] and Andrey L. Rogach*[e]

Received 4th June 2012, Accepted 6th July 2012
DOI: 10.1039/c2jm33566b

Solution based self assembly of quasi one dimensional semiconductor nanostructures (nanowires) from quasi zero dimensional (quantum dots) colloidal nanocrystal building blocks has proven itself as a powerful and flexible preparation technique. Polycrystalline CdTe nanowires self assembled from light emitting thiol capped CdTe nanocrystals are the focus of this Feature Article. These nanowires represent an interesting model system for quantum dot solids, where electronic coupling between the individual nanocrystals can be optically accessed and controlled. We provide a literature based summary of the formation mechanism and the morphology related aspects of self assembled CdTe nanowires, and highlight several fundamental and application related optical properties of these nanostructures. These include fundamental aspects of polarization anisotropies in photoluminescence excitation and emission, the electronic coupling between individual semiconductor nanocrystals constituting the nanowires, and more applied, waveguiding properties of CdTe nanowire bundles and anti Stokes photoluminescence in a prototypical structure of co axial nanowires. The optical properties of self assembled CdTe nanowires considered here render them potential candidates for photonic nano scale devices.

Introduction

Semiconductor nanostructures with large aspect ratios, commonly termed nanowires (NWs) have been the focus of extensive research during the last few decades.[1–5] Their length (typically in the micrometer range) is sufficiently large for easy manipulation in combination with photolithographically created structures. This makes NWs attractive as interconnects and renders them suitable objects for studies of transport phenomena. At the same time, their small diameter of a few

[a]*Centro de Fisica de Materiales (CFM), CSIC UPV/EHU, Donostia International Physics Center (DIPC), Paseo Manuel de Lardizabal 5, Donostia San Sebastian, 20018, Spain*
[b]*IKERBASQUE, Basque Foundation for Science, Bilbao, 48011, Spain*
[c]*Photonics and Optoelectronics Group, Department of Physics and Center for Nanoscience (CeNS), Ludwig Maximilians Universitat Munchen (LMU), Amalienstr. 54, D 80799 Munich, Germany*
[d]*School of Physics and CRANN Research Centre, Trinity College Dublin, Dublin 2, Ireland*
[e]*Department of Physics and Materials Science & Centre for Functional Photonics (CFP), City University of Hong Kong, Tat Chee Avenue, Kowloon, Hong Kong S.A.R. E mail: andrey.rogach@cityu.edu.hk*

Andrey L. Rogach

Andrey L. Rogach is a chair professor at the Department of Physics and Materials Science and the founding director of the Centre for Functional Photonics at City University of Hong Kong. He received his Ph.D. in chemistry (1995) from the Belarusian State University in Minsk, and worked at the Institute of Physical Chemistry of the University of Hamburg from 1995 to 2002. From 2002 to 2009 he was a lead staff scientist at the Department of Physics of the Ludwig Maximilians Universität in Munich, where he completed his habilitation in experimental physics. His research focuses on synthesis, assembly and optical spectroscopy of colloidal semiconductor and metal nanocrystals and their hybrid structures, and their use for photovoltaics and (bio)sensing applications.

hundred nanometres down to just a few nanometers is often smaller than many important physical length scales, such as the exciton Bohr radius, exciton diffusion length, and the wavelength of light. This frequently leads to the observation of quantum confinement effects. This set of properties, combined with their intrinsic polarization anisotropies, makes semiconductor NWs very attractive for a variety of applications, ranging from field effect transistors,[6] lasers[7] and LEDs[8] to nanosensors for biological and chemical species,[9] as well as recently envisaged nanostructures for energy conversion[5] including solar cells, electrochemical energy storage, and thermoelectrics.

Different types of quasi one dimensional semiconductor nanostructures from a variety of materials can be fabricated by a number of flexible techniques. We refer the reader to the reviews by Zacharias *et al.* for vapour grown NWs,[2] Kuno for nanostructures chemically grown in solution,[4] and Xia *et al.* for the very comprehensive treatment of both.[1] Many different synthetic methods for semiconductor NW fabrication, including the conventional vapour liquid solid technique to porous anodic alumina templating approaches,[2] solution liquid solid growth,[10] utilization of soft templates[11] and virus based scaffolds[12] have been developed. Solution based self assembly of NWs from semiconductor nanocrystal (NC) building blocks takes a prominent place. The latter was pioneered particularly by the Kotov group,[3,13] and many others.[14–19] The oriented attachment of primary, often quasi zero dimensional, organic ligand capped nanoparticles, followed by fusion into crystalline NWs driven by the elimination of high energy facets is the most commonly accepted mechanism for the solution based self assembly approach.[20]

Water based CdTe NCs bearing various thiol molecules as surface ligands[21,22] are very flexible building blocks for the fabrication of self assembled solution based superstructures.[3,22] As demonstrated for the first time by Tang *et al.*,[13] the gentle removal of negatively charged thioglycolic acid (TGA) ligands through treatment with methanol causes a spontaneous self assembly of CdTe NCs into quasi one dimensional NWs. Positively charged thiol ligands on the same kind of NCs allowed for their assembly into two dimensional free floating sheets.[23] The additional action of light promoted the formation of twisted ribbons composed of partially oxidized CdS/CdTe nanoparticles.[24]

In a comprehensive set of studies conducted by Kotov and collaborators,[25–28] which included Monte Carlo simulations of self assembly of CdTe NCs into wires and sheets[27] and surrounding medium effects on CdTe NW growth,[28] it was established that the assembly of CdTe NCs into NWs is dominated by charge dipole and dipole dipole interactions between the nanoparticle building blocks. This leads to their fusion into one dimensional pearl necklace like chains and further to NWs through the mechanism of oriented attachment. It is well documented[29,30] that thiol capped CdTe NCs exhibit a cubic (zinc blende) crystal phase, which is considered to mainly form non symmetrically truncated tetrahedrons.[26] The direction of the tetrahedron's dipole depends on the number of truncations.[26] The associated dipole moments have been experimentally found to be as high as 40–60 D in zinc blende ZnSe NC.[31] At the same time, the carboxylic acid groups of the TGA ligand shell on CdTe NCs create a net negative charge reaching 2 to 10 electrons per particle.[32] This results in a large repulsive force between NCs in their original aqueous solution. Partial removal of TGA stabilizers from the NC surface due to treatment with methanol reduces the repulsive forces between NCs, causing them to form linear aggregates and later on to fuse into thicker, polycrystalline wires. The fusion can be accompanied by the recrystallization of the initially zinc blende CdTe NCs building blocks into wurtzite single crystalline CdTe NWs, occurring through the Ostwald ripening mechanism.[28] Other attractive forces involved in the formation of CdTe based NWs are van der Waals interactions and hydrogen bonding between thiol ligands.[27,28]

The formation mechanism and morphology related aspects of semiconductor NWs self assembled from CdTe NCs building blocks have been addressed in detail in many original publications of which a summary is provided above. In the remainder of this Feature Article we focus on our own work on several fundamental and application related aspects of polycrystalline CdTe NWs. We first introduce our fabrication technique of NWs in a phosphate buffer solution[15,33] and discuss the morphology of the resulting polycrystalline CdTe NWs and bundles thereof. We then address fundamental aspects of the NWs' polarization anisotropies in photoluminescence (PL) excitation and emission beyond the electrostatic limit.[34] This is followed by a discussion of different mechanisms of electronic coupling between the light emitting constituent CdTe NCs and their thermomechanical control.[33,35] Finally, we demonstrate waveguiding properties of NW bundles,[36] and show the possibility of anti Stokes PL in a prototypical structure of co axial CdTe NW self assembled from nanoparticles of two different sizes.

Formation of CdTe NWs and bundles thereof induced by treatment of CdTe NCs with a phosphate buffer solution

Polycrystalline CdTe NWs, or bundles thereof, can be prepared from CdTe NCs building blocks *via* treatment of colloidal solution with a phosphate buffered saline (PBS) solution.[15] CdTe NCs are synthesized as reported in ref. 30 using TGA as a short chain capping ligand, with its thiol group being connected to the NC surface and the protonated carboxylic groups providing net negative charge in their native aqueous environment. Upon PBS treatment, CdTe NCs arrange into pearl necklace like agglomerates (Fig. 1a–c) within 10–15 min of growth, due to the screening of the negative surface charge of nanoparticles (provided by carboxylic acid groups of TGA capping ligands) by ions present in the phosphate buffer solution,[33] as well as the partial removal of TGA molecules from the CdTe NCs surfaces.[15] Fluorescence lifetime imaging microscopy (FLIM) of pearl necklace agglomerates of CdTe NCs (Fig. 1d) reveals strong variations of PL lifetimes along the chains, which is consistent with the previously reported one dimensional energy transfer between the neighboring CdTe NCs.[25] The FLIM image further indicates that the nanoparticle chains are rather flexible and thus in an early assembly stage with probably still significant amounts of ligands around the individual NC building blocks. The cartoon in Fig. 1a illustrates that the internal structure of these chains are composed of loosely packed individual CdTe NCs.

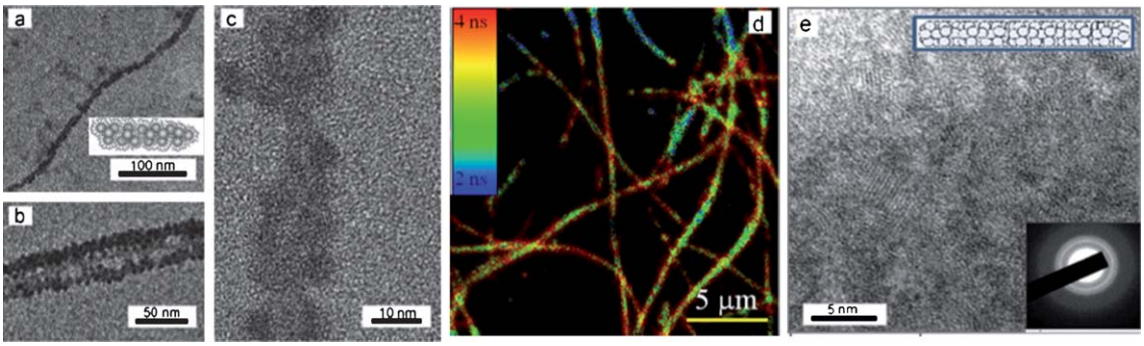

Fig. 1 (a and b) Representative TEM and (c) high resolution TEM images of the pearl necklace like chains formed at the initial stages (15 min) of CdTe NW growth in PBS solution. Reproduced with permission from ref. 33, Copyright 2007 ACS. (d) FLIM image of CdTe pearl necklace like chains. (e) High resolution TEM image illustrating the polycrystalline nature of the aged (3 days growth) CdTe NWs; individual NCs with different orientations of their lattice planes are easily recognizable. The inset in (e) displays an electron diffraction pattern of the polycrystalline single wire. Courtesy of Dr M. Doblinger, LMU. The cartoons in (a) and (e) illustrate the internal structure of the CdTe NWs composed of loosely packed individual CdTe NCs at the initial stage of their formation (a) and of the closely packed NCs with partially removed surface ligands in aged NWs (e).

As outlined in the previous publication,[33] FLIM measure ments revealed different lifetime kinetics in intercrossed and branched NWs. The most remarkable difference is the strong suppression of the long lifetime component in the branching region which is accompanied by reduction in the emission intensity. For the intercrossed region, the lifetime dynamics are very similar to the rest of the straight NW, showing that although these are crossed there is little or no energy transfer occurring between the wires. On the other hand, the sharp reduction in the PL intensity and the shortening of the lifetime give strong evidence for energy transfer in the branched region.

Compared with the emission of CdTe NCs building blocks in the aqueous solution, the PL peak of CdTe NCs pearl necklace like chains shows an 8 nm red shift and a slight decrease in PL linewidth (Fig. 2a). At the same time the PL lifetime decreases (Fig. 2b). The red shift generally originates from the coupling of electron and hole wavefunctions of neighboring NCs in the NW, and can be explained in terms of two different mechanisms: (i) the transition from electronic states of individual NCs to collective states that are delocalized over at least a fraction of the NCs constituting the NW[37,38] and (ii) dipole dipole interaction of the adjacent particles that allow for resonant energy transfer between NCs in the NW.[25,39,40] The observed red shift of PL peak combined with narrowing of the PL linewidth in CdTe NC chains is consistent with the process of long range resonance energy transfer through dipole dipole interparticle interactions funneling the energy into low energy sites (*i.e.* largest NCs) in the NW.[25,33] At the same time, the rather symmetric shape of the shifted emission peak with no prominent short or long wave length features indicates that delocalization of electron and hole wavefunctions over several NCs does not play the dominant role here, *i.e.* the electronic coupling between NCs in the pearl necklace like agglomerates is weak. This is in contrast to the much stronger electronic coupling observed as a PL broadening and the larger spectral red shifts in aged CdTe NWs, which we will address in detail in the section on CdTe quantum dot NW solids below.

In a typical synthesis of aged CdTe NWs, PBS solution is mixed with 0.01 mM (particle concentration) colloidal solution of the CdTe NCs, and the mixture is kept in the dark for 3 days until the formation of a precipitate occurs. The precipitate con taining CdTe NWs is separated from supernatant by centrifu gation and re dispersed in de ionized water. Typical CdTe NWs formed as a result of this growth technique are illustrated by

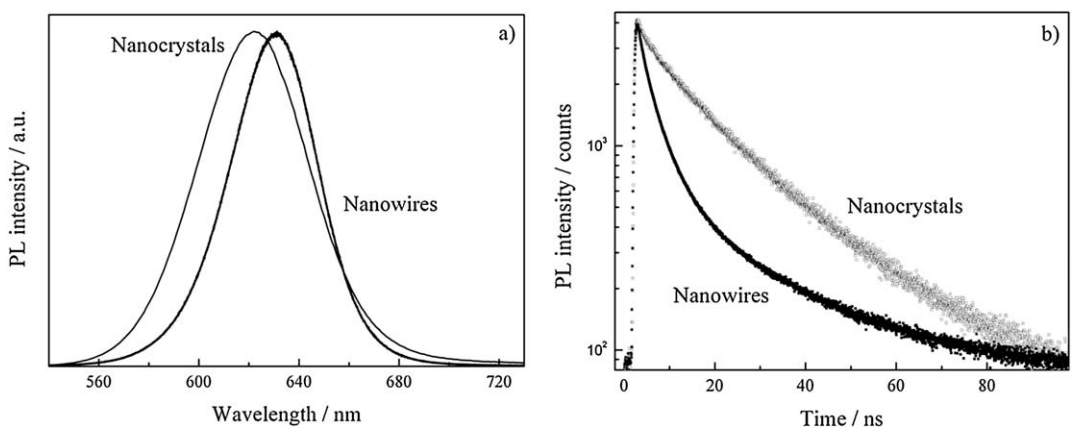

Fig. 2 (a) Normalized PL spectra and (b) PL decays of CdTe NCs in solution and of CdTe NWs grown thereof. Decay time changes from 14.4 ns for NCs to 1.9 ns for NW. Reproduced with permission from ref. 33, Copyright 2007 ACS.

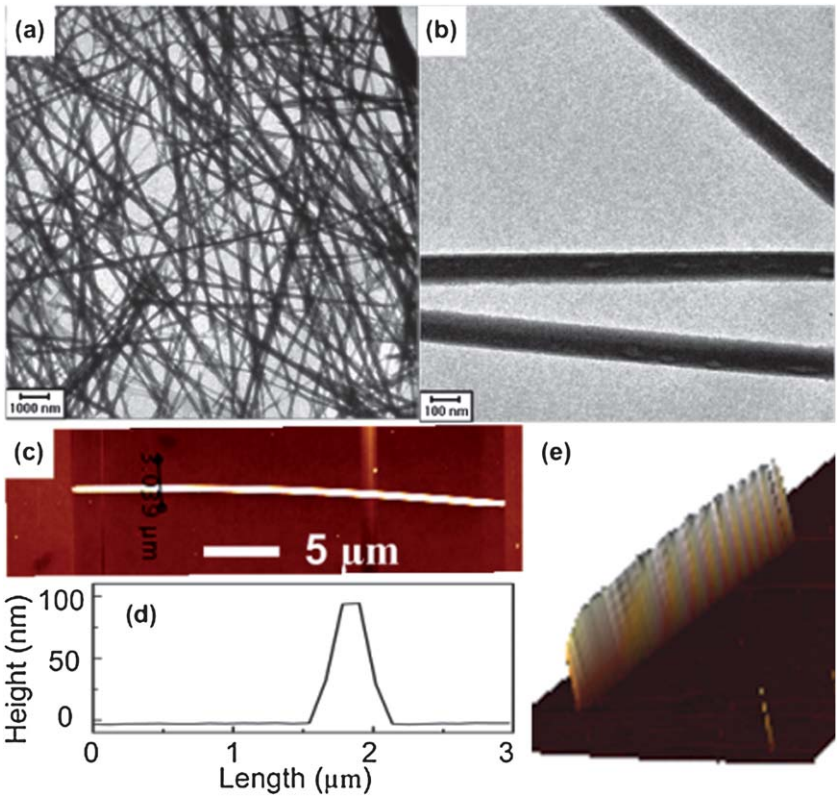

Fig. 3 (a and b) Representative TEM images of CdTe NWs; (c) AFM image of a single CdTe NW; (d) cross section along the NW presented in AFM image (c) and (e) 3D AFM topographic image of the CdTe NWs from the panel (c).

TEM images in Fig. 3a and b and an AFM image in Fig. 3c. The NWs have a typical length of several tens of micrometers; both TEM images and AFM height profiles (Fig. 3d and e) demonstrate their high uniformity along the long axis. The diameter of the NWs can be controlled by tuning the ratio between the NCs and PBS: upon changing the volume ratio from 3 : 1 to 1 : 1, the average diameter of CdTe NWs decreases from 110 to 40 nm, respectively.

The re crystallization of initially cubic (zinc blende phase) CdTe NCs into single crystalline wurtzite phase NWs, as reported by Kotov *et al.*, takes place on a time scale of several weeks.[13,28] Thus, re crystallization was not observed under our much faster growth conditions (3 days) with the PBS treatment. The aged CdTe NWs considered here still consist of zinc blende phase CdTe NCs building blocks, as evidenced by the HRTEM image in Fig. 1e. This means that the NWs discussed here are polycrystalline, *i.e.* they consist of individual closely packed CdTe NCs separated by residual organic ligands, as illustrated by the cartoon in Fig. 1e.

For some batches of NWs produced by the PBS treatment of CdTe NC solutions, formation of NW bundles has been observed. The bundles have a width of 100 to 500 nm and a height of 30 to 80 nm; they possess a roughly rectangular cross section and consist of parallel oriented NWs with diameters between 20 and 40 nm (Fig. 4). The formation process of the bundles involves two steps: the previously outlined NW growth *via* oriented attachment of individual CdTe NCs and, secondly, bundle formation *via* lateral attachment of the NW. Once formed, the NWs can, if their surface charge (and therefore mutual Coulomb repulsion) is low enough, laterally attach to form bundles in order to minimize the overall free energy of the system. Here as well, van der Waals interactions will play the dominant role. This process occurs spontaneously under ambient conditions. The size, structure, and surface charge of NWs prepared by oriented attachment depend on how fast and how much of the TGA ligands are screened/removed by PBS treatment, which, in turn, depends on the amount of ligands present on the original CdTe NCs. The latter parameter, however, is not readily controlled for the original NCs and may vary from batch to batch undergoing post preparative size selective precipitation and re dispersion steps.[30] This is consistent with the fact that we observe bundle formation in some NC batches while in others, under the same conditions of PBS treatment, only NWs are formed. We therefore attribute the bundle formation to batches of starting NCs material with particularly low surface charges.

Polarization anisotropies of self-assembled CdTe NWs beyond the electrostatic limit

Semiconductor NWs are generally known for their strongly anisotropic optical properties including absorption, PL and photoconduction.[41,42] NWs with diameters much smaller than the wavelength of the absorbed, emitted, or scattered light can be described in the electrostatic limit, *i.e.* by only taking into account the contrast in the dielectric constant between the NW and the surrounding medium.[43] However, for NW diameters comparable to the wavelength of light, non trivial diameter dependent effects can be expected.[44–46] We have used

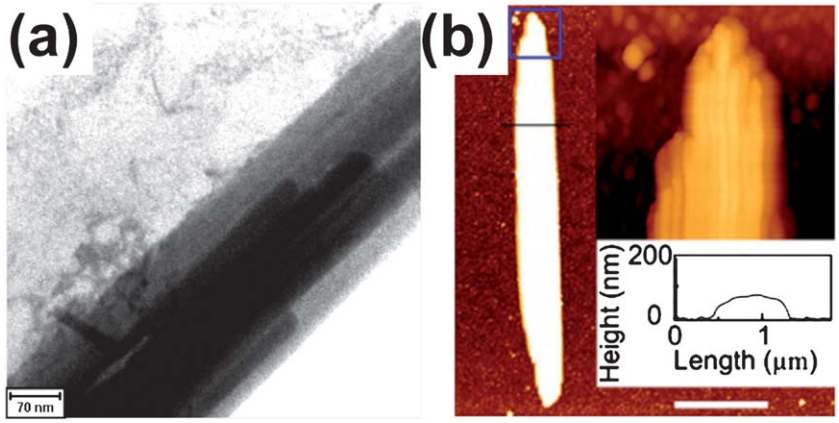

Fig. 4 (a) TEM image and (b) scanning force microscopy image of a CdTe NWs bundle. The insets in (b) show a zoom in into the area marked with the blue square and a line profile along the black line, respectively. Scale bar in (b) is 2 μm. Part (b) is reproduced with permission from ref. 36, Copyright 2010 AIP.

self assembled CdTe NWs of ~90 nm diameter to investigate this interesting size regime between ultrathin NWs and bulk materials.[34] Fig. 5 illustrates the polarization anisotropy in PL excitation and emission, as well as white light Rayleigh scattering for an individual CdTe NW. Clearly, strong polarization anisotropies are observed. However, the signal modulation is significantly lower than 100%, while the electrostatic model predicts polarization anisotropies in excess of 0.9. This shows that indeed the electrostatic approximation breaks down in this diameter range. Apparently, from Fig. 5, the polarization anisotropies, or modulation depths, are different if the polarizer is placed in the excitation or detection path, respectively. In addition, Rayleigh scattering displays slightly different polarization anisotropies compared to PL.

Employing finite difference time domain (FDTD) calculations, which take into account the finite diameter of the NWs, these observations can be explained. Fig. 5 displays calculated polarization anisotropies for polarized excitation at 400 nm and polarized detection at 600 nm wavelength as a function of the NW diameter wavelength ratio. In both cases, the prediction of the electrostatic limit is reproduced at small diameter wavelength ratios. At a critical ratio close to 0.1, which is larger for polarized detection, first a slight increase followed by a sharp decrease in the polarization anisotropy is observed. This clearly demonstrates that the reduced polarization anisotropies observed experimentally are due to the finite diameter of the NWs and that a regime beyond the electrostatic limit is reached. Furthermore, the calculations show that tuning the diameter of the CdTe NWs allows for controlling the polarization anisotropies from their maximum value all the way to zero. The calculations also reproduce the experimental observation that in polarized detection, the polarization anisotropies are larger. This can be mainly attributed to dispersion, *i.e.* the fact that the dielectric constant decreases when going from 400 nm (polarized excitation) to 600 nm (polarized detection). This change in wavelength also changes the effective "optical diameter" of the NW.

The polarization anisotropies of individual NWs in PL excitation and emission, and scattering can be transferred to oriented NWs ensembles in stretched polymer films.[34] In that case, a decrease in polarization anisotropy due to a reduced "dielectric contrast" in the polymer matrix is counterbalanced by multiple scattering, which increases polarization anisotropies. This opens opportunities for the application of self assembled NWs in polarization sensitive applications.

Thermomechanically controlled electronic coupling in a CdTe quantum dot NW solid

The polycrystallinity of self assembled aged CdTe NWs renders them interesting model systems for quantum dot solids.[39] This allows insight to be gained into the electronic coupling between the individual NCs in such a structure. Generally, NCs in close proximity couple electronically due to spatial overlap of the electronic wavefunctions of neighboring particles. This leads to delocalization of electronic states across several semiconductor quantum dots and, in the case of highly ordered systems, to the formation of minibands.[37] It should be noted, that the coupling is strongly distance dependent.[47] Optically, delocalized electronic states are observed as a red shifted transition when compared with isolated semiconductor NCs.[48] As opposed to the case of the PL of the CdTe pearl necklace like chains (Fig. 2), the PL of the aged CdTe NWs is strongly red shifted not only in comparison to the well separated CdTe NCs dispersed in polymer matrix, but also compared to the closely packed NC films with completely intact TGA ligand shells (Fig. 6). At the same time, the PL spectrum of the NW exhibits strong, symmetric broadening. This indicates stronger electronic coupling and larger electronic disorder in CdTe NWs as compared to CdTe pearl necklace like chains, where the delocalization of electron and hole wavefunctions over several NCs was found to be less important.[35]

In polycrystalline CdTe NWs formed *via* self assembly, the interstitial space between particles is still filled with residual TGA ligands. This gives rise to a unique temperature dependence of the PL in these NWs.[35] While isolated CdTe NCs well dispersed in an inert polymer matrix, as well as CdTe bulk material exhibit a well known PL blue shift when cooled to 5 K,[49] polycrystalline NWs from the same CdTe NCs exhibit a red shift in PL when cooled to the same temperature (Fig. 6). This behavior can be explained by a dominating effect of the NW shrinking at low

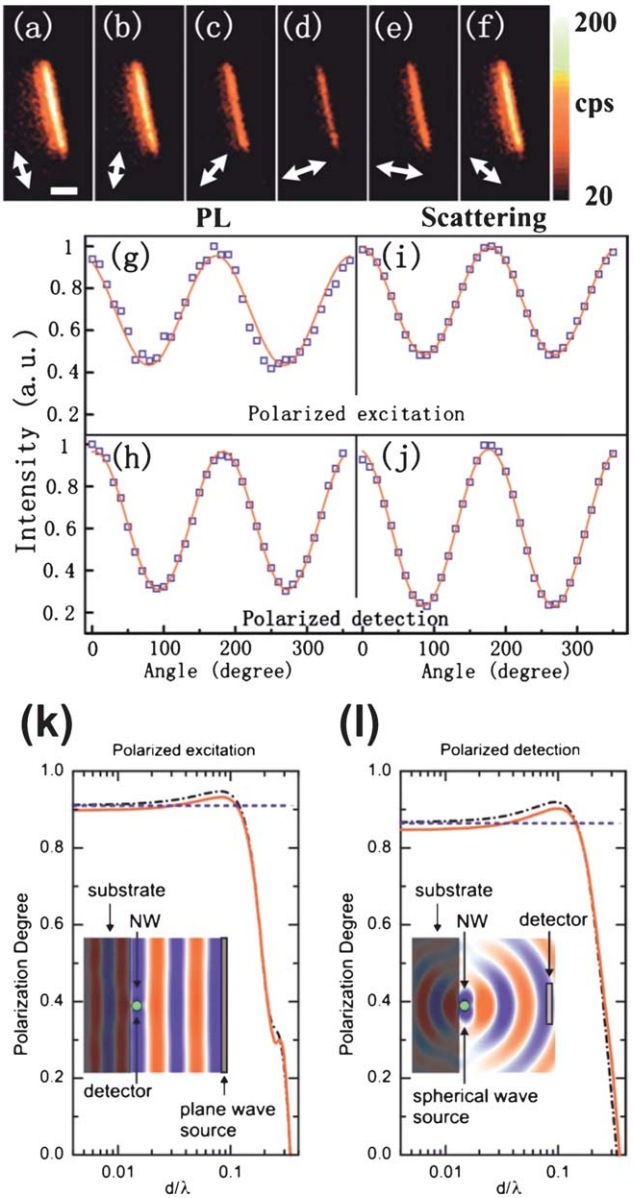

Fig. 5 (a f) PL images of an individual CdTe NW with the excitation polarization indicated by the white arrow. Scale bar is 5 μm. (g j) Polarization dependence of PL and scattering of the same NW as function of angle with respect to the NW long axis with the polarizer placed in the excitation and detection path, respectively. Solid lines are best fits to $\sin^2$ functions. (k and l) Polarization degrees of the PL as function of diameter to wavelength ratio calculated for polarized excitation and polarized detection, respectively. Insets illustrate the simulated geometries. Dashed lines represent the electrostatic limit, dash dot lines represent an isolated NW, and the solid lines represent a NW on a substrate. Reproduced with permission from ref. 34, Copyright 2010 APS.

temperatures. Upon cooling, both CdTe NCs and the residual organic ligands shrink, which reduces the size of the NW. While the shrinking of the individual NCs would lead to a PL blue shift, the shrinking of the TGA ligand molecules reduces the interparticle distance, which results in a larger electronic coupling between the NCs leading to a red shift in PL. In the case of a sub nanometer distance between the CdTe NCs (Fig. 1e) the effect of the reduced interparticle distance dominates and an overall red

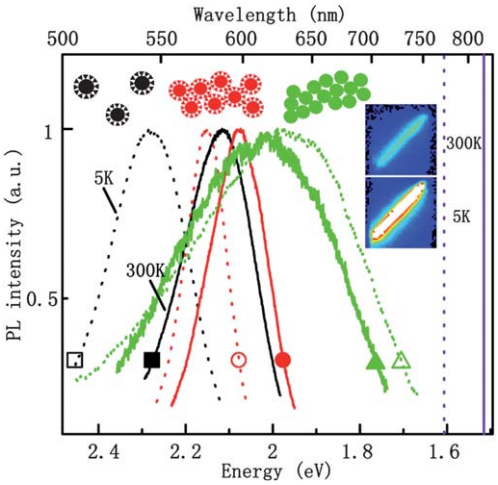

Fig. 6 PL spectra of well separated CdTe NCs in a polymer matrix (black, square), closely packed CdTe NCs films with intact ligand shells (red, circles) and an individual polycrystalline CdTe NW comprising CdTe NC with residual TGA ligands (green, triangle). Solid (full symbol) and dotted (open symbol) lines represent PL at room temperature and 5 K, respectively. The band gap energies of bulk CdTe of 1.51 eV and 1.61 eV at room temperature and 5 K are indicated as vertical lines. The inset shows the PL images of an individual CdTe NW at room temperature and 5 K (image size 17.5 × 17.5 μm^2). Reproduced with permission from ref. 35, Copyright 2010 AIP.

shift is observed for the polycrystalline CdTe NWs upon cooling. The temperature induced PL red shift observed in CdTe NWs is absent in both isolated CdTe NCs and CdTe bulk material. It must therefore be considered a novel effect arising only in the hybrid organic semiconductor material. This opens new opportunities in controlling the temperature dependence of the material. In particular, designing a hybrid material with a temperature independent band gap seems possible.

Waveguiding properties of CdTe NW bundles

The quasi one dimensional nature of semiconductor NWs, their large refractive index when compared with organic materials, and the cheap and fast solution processing technique employed for their synthesis and assembly renders them attractive candidates for sub wavelength waveguides. This is interesting for future information technology which is expected to feature highly integrated photonic and optoelectronic components on a single chip.[50] We employed self assembled CdTe NW bundles to study their waveguiding properties.[36] Fig. 7 displays Rayleigh scattering and laser excitation PL images of individual NW bundles. Clearly, the PL is not emitted from the location of the laser excitation, but from the end of the NW bundle. Thus the PL couples into a guided mode of the NW bundle, and propagates to the bundle end where it is emitted. Apparently, waveguiding occurs over distances of several micrometers. Varying the position of the laser excitation while monitoring the emitted PL intensity at the bundle's end allows for estimating the losses in the NW bundle waveguide to be on the order of ~3.9 dB μm^{-1}.[36] This is larger than for single crystalline NWs (due to more defects that allow for scattering) but is comparable to a single metal strip plasmonic waveguide.[51,52]

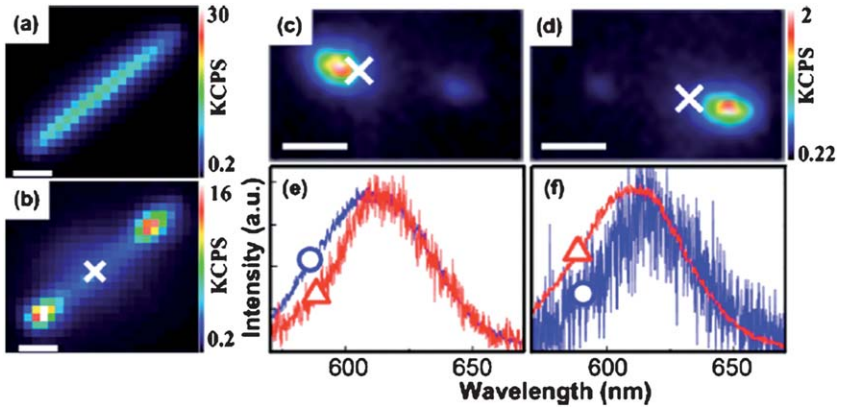

Fig. 7 (a) Scattering and (b d) PL images of individual CdTe NW bundles. The white cross indicates the location of laser excitation. (e and f) Normalized PL spectra obtained from the left (blue circle) and right (red triangle) ends of the NW bundle in (c) and (d), respectively, demonstrating the reabsorption of PL in the NW bundle. Scale bars are 1 μm (a and b) and 2 μm (c and d), respectively. Reproduced with permission from ref. 36, Copyright 2010 AIP.

The losses in the CdTe NW bundle are dominated by reab sorption of the PL by the constituting NCs. This is evidenced by the comparison of the PL spectra at the two bundle ends under asymmetric laser excitation, *i.e.* not in the bundle center (Fig. 7). The emission at the farther end displays a reduced intensity at the blue edge of the emission spectrum. This part of the emission has a larger overlap with the NC's absorption and is therefore more strongly reabsorbed. In addition, simple geometric arguments, assuming a rectangular cross section of the bundle, suggest that the smallest bundles investigated (width of 170 nm) act as a single mode waveguide, since they are too narrow to support higher order guided modes.

Co-axial core–shell CdTe NWs employing CdTe NCs of two different sizes

The fabrication of NW heterostructures using colloidal chem istry techniques is expected to create new platforms for designing materials and devices with diverse functions.[3] In a proof of concept study, we grew co axial NW heterostructures combining CdTe NCs of two different sizes. The main idea behind this approach is to take advantage of the size dependent bandgap tuning in semiconductor NCs and, at the same time, to avoid complications caused by lattice mismatches.[53,54] Strong anti Stokes emission from these NWs was observed using low inten sity below band gap excitation.

The NWs grown for 24 h from small CdTe NCs (2.8 nm mean diameter, PL maximum at 570 nm) as outlined in the previous section provided the core NWs for further treatment. They were immersed in a solution of bigger CdTe NCs (3.5 nm size, PL maximum at 610 nm) and allowed to further grow for 2 days. Fig. 8 shows the PL spectrum measured with a confocal setup from an individual core NW composed from the 2.8 nm NCs (curve 1) in comparison with the PL spectrum of the 3.5 CdTe NCs in solution (curve 2), together with the PL spectrum of an individual core shell NW formed after the treatment of the core NW in a solution of 3.5 nm CdTe NCs (curve 3). The emission maximum of the latter is red shifted with respect to both the emission maximum of the original core NW and the PL band of the 3.5 nm CdTe NCs in colloidal solution. The latter 12 nm shift indicates that the NCs form a close packed shell on the core wire which results in a decreased electronic confinement in the shell. The inset in Fig. 8 demonstrates the high uniformity of the resulting co axial structure. The PL spectrum of the individual co axial NW (Fig. 8, curve 3) also possesses a small shoulder in the wavelength region of the PL peak of the original core wire, revealing that we have combined emission from the smaller NCs forming the core and the bigger NCs forming the shell of the co axial structure. These spectroscopic results provide the evidence of the feasibility of co axial semiconductor heterostructures self assembled in solution, avoiding the use of bio conjugation

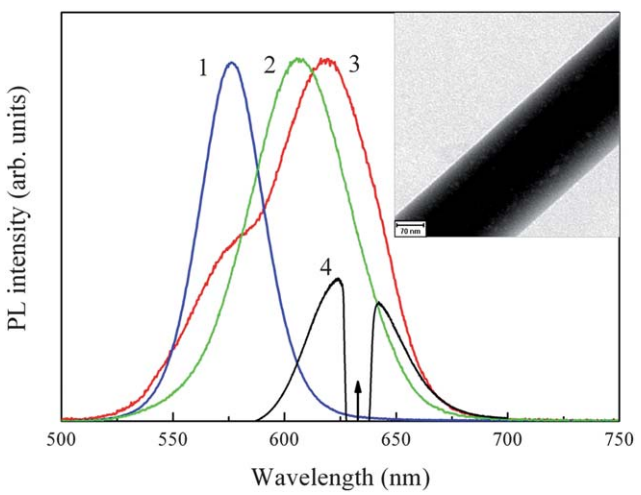

Fig. 8 PL spectrum of the core NW grown from 2.8 nm CdTe NCs (curve 1) in comparison to the PL spectrum of an aqueous dispersion of the 3.5 nm CdTe NCs (curve 2), and the PL spectrum of the co axial core shell CdTe NWs (curve 3). All PL spectra were recorded using excitation at 488 nm on a RENISHAW micro PL set up allowing for measurements on single NWs. Curve 4 shows anti Stokes emission from a single core shell CdTe NWs recorded under excitation at 632.8 nm (as indicated by arrow). The dip in the lineshape of curve 4 is a result of the use of a notch filter to eliminate the excitation line from the detection channel. The inset shows a TEM image of a co axial core shell CdTe NWs.

strategies previously employed for the growth of co axial semi conductor core semiconductor (or metal) shell NWs.[40,55]

Along with other applications of semiconductor NCs, optical cooling promoted by their anti Stokes PL has been recently proposed.[56] This type of emission process involves the emission of higher energy photons than those that are absorbed. The absorption of vibrational energy distinguishes anti Stokes PL from other up conversion effects like two photon or two step excited luminescence. As a result, the intensity of the anti Stokes PL abnormally increases with temperature by gaining energy from the thermal bath in contrast to the conventional quenching of resonant or Stokes shifted PL with increasing temperature.[57] To provide excitation in the anti Stokes regime, we recorded a PL spectrum of a single co axial CdTe NW using below band gap excitation by a HeNe laser emitting at 632.8 nm. The anti Stokes PL is shown in Fig. 8, curve 4, with its tail extending up to ~300 meV above the excitation energy. The anti Stokes PL is red shifted with respect to PL maximum of the Stokes shifted PL (Fig. 8, curve 3). This red shift is a result of size selective exci tation within the population of NCs forming NWs.[57] When the excitation is restricted to the onset region of the absorption spectra, then NCs of a much narrower size range are excited, which are the largest in the ensemble. The anti Stokes PL process is highly efficient having an intensity comparable to the Stokes PL from the same wire shown in Fig. 8, curve 3. The integrated intensity of the anti Stokes PL in co axial CdTe NWs has an almost linear dependence on the excitation intensity under weak or moderate excitation (<200 W cm^{-2}), which is very similar to the behavior of anti Stokes PL in colloidal CdTe NCs where the progressive transition from Stokes PL into anti Stokes PL can be observed when changing the excitation wavelength to below the band gap region.[56,57]

Conclusions and outlook

For the last few decades, in the quest for quasi one dimensional semiconductor nanostructures, researchers have increasingly addressed their preparation *via* self assembly from solution based nanoparticle building blocks. This concept is now widely recognized as a very powerful and flexible tool of bottom up nanotechnology. The unique advantage of self assembled CdTe nanostructures is their template free, fast solution based growth at room temperature where the use of different organic capping ligands on the constituting CdTe NCs building blocks determine their resulting morphology, ranging from one dimensional NWs to twisted ribbons and two dimensional sheets. The ability to tune the emission wavelength of NWs by the size of the utilized semiconductor NC building blocks makes self assembled CdTe NWs interesting candidates for a variety of photonic and opto electronic devices. Polycrystalline self assembled CdTe NWs are interesting model systems for quantum dot solids, where elec tronic coupling between the individual NCs can be accessed and controlled. We have summarized the existing knowledge on the formation mechanism and the morphology related aspects of the self assembled CdTe NWs, and provided an overview of several fundamental and application related optical properties of these nanostructures. In particular, polarization anisotropies in PL excitation and emission of the NWs beyond the electrostatic limit, and the electronic coupling between the light emitting CdTe NCs constituting the wires have been addressed. We further demonstrated thermomechanical control of electronic coupling in quantum dot NWs solids, and showed the possibility of anti Stokes emission in prototypical co axial NWs. The latter is potentially promising for laser cooling applications. Self assembled CdTe NWs bundles act as sub wavelength single mode waveguides in the red visible spectral range with losses comparable to single metal strip plasmonic waveguides. This renders them potential candidates for short range optical inter connects in future integrated photonic and optoelectronic circuits. A key area of active research will involve the directed assembly of oriented arrays of NWs for applications in energy harvesting structures. Taken as a whole, the optical properties of self assembled CdTe NWs make them potential building blocks for faster and smaller next generation photonic and optoelec tronic nano scale devices.

Acknowledgements

The authors are deeply indebted to all the colleagues and collaborators who have contributed to the work on semi conductor nanowires discussed in this article, and in particular to Jianhong Zhang, Andrey A. Lutich, Andrei S. Susha, Markus Döblinger, Matthias Gerlach, and Jochen Feldmann. This research was supported by the German Research Foundation (DFG) *via* the "Nanosystems Initiative Munich (NIM)", by the ETORTEK 2011 2013 project "nanoIKER" from the Depart ment of Industry of the Basque Government, by Science Foun dation Ireland under the PI programme, grant number 08/IN.1/ I1862, and by the Research Grant Council of Hong Kong S.A.R. (project no. [T23 713/11]).

References

1 Y. N. Xia, *et al.*, One dimensional nanostructures: synthesis, characterization, and applications, *Adv. Mater.*, 2003, **15**(5), 353 389.
2 H. J. Fan, P. Werner and M. Zacharias, Semiconductor nanowires: from self organization to patterned growth, *Small*, 2006, **2**(6), 700 717.
3 Z. Y. Tang and N. A. Kotov, One dimensional assemblies of nanoparticles: preparation, properties, and promise, *Adv. Mater.*, 2005, **17**(8), 951 962.
4 M. Kuno, An overview of solution based semiconductor nanowires: synthesis and optical studies, *Phys. Chem. Chem. Phys.*, 2008, **10**(5), 620 639.
5 A. I. Hochbaum and P. D. Yang, Semiconductor nanowires for energy conversion, *Chem. Rev.*, 2010, **110**(1), 527 546.
6 X. F. Duan, *et al.*, Indium phosphide nanowires as building blocks for nanoscale electronic and optoelectronic devices, *Nature*, 2001, **409**(6816), 66 69.
7 X. F. Duan, *et al.*, Single nanowire electrically driven lasers, *Nature*, 2003, **421**(6920), 241 245.
8 Y. Huang, X. F. Duan and C. M. Lieber, Nanowires for integrated multicolor nanophotonics, *Small*, 2005, **1**(1), 142 147.
9 Y. Cui, *et al.*, Nanowire nanosensors for highly sensitive and selective detection of biological and chemical species, *Science*, 2001, **293**(5533), 1289 1292.
10 T. J. Trentler, *et al.*, Solution liquid solid growth of crystalline III V semiconductors an analogy to vapor liquid solid growth, *Science*, 1995, **270**(5243), 1791 1794.
11 L. Zhang, *et al.*, Branched wires of CdTe nanocrystals using amphiphilic molecules as templates, *Small*, 2005, **1**(5), 524 527.
12 C. B. Mao, *et al.*, Virus based toolkit for the directed synthesis of magnetic and semiconducting nanowires, *Science*, 2004, **303**(5655), 213 217.

13 Z. Y. Tang, N. A. Kotov and M. Giersig, Spontaneous organization of single CdTe nanoparticles into luminescent nanowires, *Science*, 2002, **297**(5579), 237 240.
14 C. Pacholski, A. Kornowski and H. Weller, Self assembly of ZnO: from nanodots, to nanorods, *Angew. Chem., Int. Ed.*, 2002, **41**(7), 1188 1191.
15 Y. Volkov, *et al.*, *In situ* observation of nanowire growth from luminescent CdTe nanocrystals in a phosphate buffer solution, *ChemPhysChem*, 2004, **5**(10), 1600 1602.
16 K. S. Cho, *et al.*, Designing PbSe nanowires and nanorings through oriented attachment of nanoparticles, *J. Am. Chem. Soc.*, 2005, **127**(19), 7140 7147.
17 H. Zhang, *et al.*, Manipulation of aqueous growth of CdTe nanocrystals to fabricate colloidally stable one dimensional nanostructures, *J. Am. Chem. Soc.*, 2006, **128**(31), 10171 10180.
18 C. O'Sullivan, *et al.*, Spontaneous room temperature elongation of CdS and Ag(2)S nanorods *via* oriented attachment, *J. Am. Chem. Soc.*, 2009, **131**(34), 12250 12257.
19 J. Yang, *et al.*, Self reorganization of CdTe nanoparticles into near infrared $Hg(1-x)Cd(x)Te$ nanowire networks, *Chem. Mater.*, 2009, **21**(14), 3177 3182.
20 Q. Zhang, S. J. Liu and S. H. Yu, Recent advances in oriented attachment growth and synthesis of functional materials: concept, evidence, mechanism, and future, *J. Mater. Chem.*, 2009, **19**(2), 191 207.
21 A. L. Rogach, *et al.*, Aqueous synthesis of thiol capped CdTe nanocrystals: state of the art, *J. Phys. Chem. C*, 2007, **111**(40), 14628 14637.
22 N. Gaponik and A. L. Rogach, Thiol capped CdTe nanocrystals: progress and perspectives of the related research fields, *Phys. Chem. Chem. Phys.*, 2010, **12**(31), 8685 8693.
23 Z. Y. Tang, *et al.*, Self assembly of CdTe nanocrystals into free floating sheets, *Science*, 2006, **314**(5797), 274 278.
24 S. Srivastava, *et al.*, Light controlled self assembly of semiconductor nanoparticles into twisted ribbons, *Science*, 2010, **327**(5971), 1355 1359.
25 Z. Y. Tang, *et al.*, Simple preparation strategy andone dimensional energy transfer in CdTe nanoparticle chains, *J. Phys. Chem. B*, 2004, **108**(22), 6927 6931.
26 S. Shanbhag and N. A. Kotov, On the origin of a permanent dipole moment in nanocrystals with a cubic crystal lattice: effects of truncation, stabilizers, and medium for CdS tetrahedral homologues, *J. Phys. Chem. B*, 2006, **110**(25), 12211 12217.
27 Z. L. Zhang, *et al.*, Simulations and analysis of self assembly of CdTe nanoparticles into wires and sheets, *Nano Lett.*, 2007, **7**(6), 1670 1675.
28 G. D. Lilly, *et al.*, Media effect on CdTe nanowire growth: mechanism of self assembly, Ostwald ripening, and control of NW geometry, *J. Phys. Chem. C*, 2008, **112**(2), 370 377.
29 A. L. Rogach, *et al.*, Synthesis and characterization of thiol stabilized CdTe nanocrystals, *Ber. Bunsen Ges.*, 1996, **100**(11), 1772 1778.
30 N. Gaponik, *et al.*, Thiol capping of CdTe nanocrystals: an alternative to organometallic synthetic routes, *J. Phys. Chem. B*, 2002, **106**(29), 7177 7185.
31 M. Shim and P. Guyot Sionnest, Permanent dipole moment and charges in colloidal semiconductor quantum dots, *J. Chem. Phys.*, 1999, **111**(15), 6955 6964.
32 A. A. Yaroslavov, *et al.*, What is the effective charge of TGA stabilized CdTe nanocolloids?, *J. Am. Chem. Soc.*, 2005, **127**(20), 7322 7323.
33 Y. P. Rakovich, *et al.*, CdTe nanowire networks: fast self assembly in solution, internal structure, and optical properties, *J. Phys. Chem. C*, 2007, **111**(51), 18927 18931.
34 J. Zhang, *et al.*, Optical anisotropy of semiconductor nanowires beyond the electrostatic limit, *Phys. Rev. B: Condens. Matter Mater. Phys.*, 2010, **82**(15), 155301.
35 J. H. Zhang, *et al.*, Thermomechanical control of electronic coupling in quantum dot solids, *J. Appl. Phys.*, 2010, **107**(12), 123516.
36 J. Zhang, *et al.*, Single mode waveguiding in bundles of self assembled semiconductor nanowires, *Appl. Phys. Lett.*, 2010, **97**(22), 221915.
37 M. V. Artemyev, *et al.*, Evolution from individual to collective electron states in a dense quantum dot ensemble, *Phys. Rev. B: Condens. Matter*, 1999, **60**(3), 1504 1506.
38 M. V. Artemyev, *et al.*, Spectroscopic study of electronic states in an ensemble of close packed CdSe nanocrystals, *J. Phys. Chem. B*, 2000, **104**(49), 11617 11621.
39 C. R. Kagan, C. B. Murray and M. G. Bawendi, Long range resonance transfer of electronic excitations in close packed CdSe quantum dot solids, *Phys. Rev. B: Condens. Matter*, 1996, **54**(12), 8633 8643.
40 J. Lee, A. O. Govorov and N. A. Kotov, Bioconjugated superstructures of CdTe nanowires and nanoparticles: multistep cascade Forster resonance energy transfer and energy channeling, *Nano Lett.*, 2005, **5**(10), 2063 2069.
41 C. Mauser, *et al.*, Anisotropic optical emission of single CdSe/CdS tetrapod heterostructures: evidence for a wavefunction symmetry breaking, *Phys. Rev. B: Condens. Matter Mater. Phys.*, 2008, **77**(15), 153303.
42 J. F. Wang, *et al.*, Highly polarized photoluminescence and photodetection from single indium phosphide nanowires, *Science*, 2001, **293**(5534), 1455 1457.
43 L. D. Landau, E. M. Lifshitz and L. P. Pitaevskii, *Electrodynamics of Continuous Media*, Pergamon Press, 1984.
44 H. E. Ruda and A. Shik, Polarization sensitive optical phenomena in thick semiconducting nanowires, *J. Appl. Phys.*, 2006, **100**(2), 024314.
45 J. Giblin, V. Protasenko and M. Kuno, Wavelength sensitivity of single nanowire excitation polarization anisotropies explained through a generalized treatment of their linear absorption, *ACS Nano*, 2009, **3**(7), 1979 1987.
46 L. Y. Cao, B. Nabet and J. E. Spanier, Enhanced Raman scattering from individual semiconductor nanocones and nanowires, *Phys. Rev. Lett.*, 2006, **96**(15), 157402.
47 H. Dollefeld, H. Weller and A. Eychmuller, Semiconductor nanocrystal assemblies: experimental pitfalls and a simple model of particle particle interaction, *J. Phys. Chem. B*, 2002, **106**(22), 5604 5608.
48 R. Koole, *et al.*, Electronic coupling and exciton energy transfer in CdTe quantum dot molecules, *J. Am. Chem. Soc.*, 2006, **128**(32), 10436 10441.
49 G. L. Bayatian, *et al.*, CMS physics technical design report, volume II: physics performance, *J. Phys. G: Nucl. Part. Phys.*, 2007, **34**(6), 995 1579.
50 P. J. Pauzauskie and P. Yang, Nanowire photonics, *Mater. Today*, 2006, **9**(10), 36 45.
51 E. Ozbay, Plasmonics: merging photonics and electronics at nanoscale dimensions, *Science*, 2006, **311**(5758), 189 193.
52 S. Lal, S. Link and N. J. Halas, Nano optics from sensing to waveguiding, *Nat. Photonics*, 2007, **1**(11), 641 648.
53 T. Franzl, *et al.*, Exciton recycling in graded gap nanocrystal structures, *Nano Lett.*, 2004, **4**(9), 1599 1603.
54 T. A. Klar, *et al.*, Super efficient exciton funneling in layer by layer semiconductor nanocrystal structures, *Adv. Mater.*, 2005, **17**(6), 769 773.
55 J. Lee, *et al.*, Bioconjugates of CdTe nanowires and Au nanoparticles: plasmon exciton interactions, luminescence enhancement, and collective effects, *Nano Lett.*, 2004, **4**(12), 2323 2330.
56 Y. P. Rakovich, *et al.*, Anti Stokes cooling in semiconductor nanocrystal quantum dots: a feasibility study, *Phys. Status Solidi A*, 2009, **206**(11), 2497 2509.
57 Y. P. Rakovich, *et al.*, Anti Stokes photoluminescence in II VI colloidal nanocrystals, *Phys. Status Solidi B*, 2002, **229**(1), 449 452.